Clinical Radiology 74 (2019) 653.e11–653.e18

Contents lists available at ScienceDirect

Clinical Radiology

journal homepage: www.clinicalradiologyonline.net

Hypervascular hepatic focal lesions on dynamic contrast-enhanced CT: preliminary data from arterial phase scans texture analysis for classification

S. Song [a,b,c], Z. Li [b], L. Niu [b], X. Zhou [b,*], G. Wang [b], Y. Gao [b], J. Wang [b], F. Liu [b], Q. Sui [b], L. Jiao [d], J. Lu [a,c,e]

[a] Department of Radiology, Xuanwu Hospital, Capital Medical University, Beijing, China
[b] Department of Radiology, The Affiliated Hospital of Qingdao University, Qingdao, China
[c] Beijing Key Laboratory of Magnetic Resonance Imaging and Brain Informatics, Beijing, China
[d] Interventional Medical Center, The Affiliated Hospital of Qingdao University, Qingdao, China
[e] Department of Nuclear Medicine, Xuanwu Hospital, Capital Medical University, Beijing, China

ARTICLE INFORMATION

Article history:
Received 29 October 2018
Accepted 16 May 2019

AIM: To investigate the ability of computed tomography texture analysis (CTTA) to distinguish different hypervascular hepatic focal lesions.

MATERIALS AND METHODS: CTTA software was used to analyse retrospectively 18 cases of focal nodular hyperplasia, 10 cases of hepatic adenoma, 20 cases of haemangioma, 20 cases of hepatocellular carcinoma, and 20 cases of hepatic metastases using arterial phase scans. A list of texture features was generated for lesion classification. Fisher's discriminant analysis (FDA) was used to construct a predictive model from these parameters and to estimate the discriminant accuracy. Receiver operating characteristic (ROC) curve analysis was used to assess the diagnostic performance of texture analysis of benign and malignant tumours.

RESULTS: Fifteen texture features were significant differences between the five different histopathological types of all lesions. The total discriminant accuracy was 69.3%, with 55.7% cross-validation accuracy. Seven texture features showed significant differences between the benign and malignant tumours. The total discriminant accuracy in the sample was 83%, with 77.3% cross-validation accuracy. The area under the ROC curve (AUROC) of united texture features was 0.927 (95% confidence interval [CI]=0.875–0.979).

CONCLUSIONS: CTTA can be used as an aid in the differential diagnosis of hypervascular solid focal hepatic lesions, especially the differential diagnosis between benign and malignant lesions.

Introduction

With advances in medical imaging equipment and development of computer-based post-processing

* Guarantor and correspondent: X. Zhou, The Affiliated Hospital of Qingdao University, Postal address: No.1677, Wu Tai Shan Road, Huangdao District, Qingdao City, Shandong Province, China. Tel.: +86 17853290618; fax: +86 0532 82919900.
E-mail address: Zhouxm@qduhospital.cn (X. Zhou).

https://doi.org/10.1016/j.crad.2019.05.010
0009-9260/

technology, medical images can now provide abundant information for the detection, diagnosis, treatment, and prognosis of diseases. At present, imaging diagnosis mainly relies on naked-eye observations by radiologists of X-ray, computed tomography (CT), magnetic resonance imaging (MRI), nuclear medicine positron-emission tomography (PET), and ultrasound (US) images. Different tissue contrast mechanisms are exploited by radiologists to identify patterns to enable diagnosis. The professional level, diagnostic experience, physical and mental condition, etc., of the radiologist can therefore affect the accuracy of the diagnosis. Additionally, radiological images contain more information than is visible to the clinician's eyes, and these "hidden" data can provide much more insight into the tissue of interest than previously thought. Many researchers have attempted quantitative analysis of radiological images of lesions, to explore the hidden information contained in images further, using mathematical algorithms, and statistical methods to reduce the chance of misdiagnosis. Thus, radiomics was born as a "new" method.[1,2] The principle underlying radiomics is that genomic and proteomics patterns can be expressed in terms of macroscopic image-based features. Preliminary results have been obtained in terms of diagnosis, differential diagnosis, assessment of prognosis, prediction of response to treatment,[3–8] laying the foundation for the development of precision medicine.

Texture analysis is a new, recently developed image post-processing technique, which is an important component of radiomics. The texture of images refers to the appearance, structure, and arrangement of the parts of an object within the image.[5] Texture features are mathematical parameters computed from the distribution of pixels, which characterise the texture type, and thus the underlying structure of the objects shown in the image.[9] In radiological images, quantitative changes in texture features can reflect the pathological changes in the organism, which is helpful for non-invasive assessment of tumour characteristics and prognosis, and has good application prospects and high application value in tumour imaging.[10]

Haemangioma, hepatic adenoma (HA), and focal nodular hyperplasia (FNH) are common benign focal lesions in the liver, while hepatocellular carcinoma (HCC) and hepatic metastasis are the most common malignant liver diseases.[11,12] At present, preoperative evaluation mostly entails a multi-phase CT enhanced scan, which contains embedded information on the vascularity and cellularity of hepatic hypervascular lesions[13–15]; however, observation of CT images with the naked eye can only present information about the density of lesions, such as the changes in tumour composition and cell density, necrosis, haemorrhage, and cystic degeneration. It fails to reflect the microscopic structure inside the tumour. When the imaging of lesions is atypical, differential diagnosis of hypervascular hepatic lesions is more difficult. Analysis of the texture features could provide primary or additional information, which is related to the biological nature of the lesions and beyond visual inspection.[16,17] In this pilot study, texture analysis of images in the arterial phase in dynamic contrast-enhanced CT of hypervascular hepatic solid focal lesions was undertaken in order to provide reference material for differential diagnosis.

Materials and methods

Patient selection

The hospital ethics committee approved this retrospective study, and the need for obtaining informed consent from patients was waived. All patients were identified by searching the electronic HIS database at the Affiliated Hospital of Qingdao University between February 2013 and October 2016. Demographic, clinical, and pathological data were collected from the electronic medical records. The CT appearance of each lesion was described in terms of the attenuation of the lesions in comparison to the surrounding normal parenchyma. Hypervascular hepatic lesions were defined as an area of hyper-attenuation, as compared to the surrounding normal liver parenchyma, including rim enhancement. Five types of hypervascular hepatic lesions were included in the present cohort, which included haemangioma, FNH, HA, HCC, and hepatic metastasis.

The inclusion criteria were as follows: (1) all lesions were histopathologically confirmed at surgery or liver percutaneous needle biopsy; (2) CT dynamic enhancement was performed $\leq$30 days before surgery or biopsy; (3) arterial hypervascular lesions in CT dynamic enhancement scans were included. The exclusion criteria were as follows: (1) cases in which histopathological results did not confirm the lesion; (2) hypovascular or iso-attenuation lesions found in arterial phase of CT dynamic enhancement scan; (3) lesions with a diameter $<$10 mm; (4) lesions with an indistinct margin (where the interface between the lesion and normal liver parenchyma was vague), making it unsuitable for outlining a region of interest (ROI); (5) images where movement or other artefacts might influence the result of texture analysis; (6) images from patients who had received any treatment for hepatic lesions before needle biopsy or surgery, such as chemotherapy, previous local regional treatment (transcatheter arterial chemoembolisation, radiofrequency ablation, etc.), or hepatic resection.

Pathological analysis

After surgery or liver percutaneous needle biopsy, the pathological results were described by the institution's pathology reports. All hepatic specimens were cut into sections with 5-mm thickness, fixed in 10% buffered formaldehyde solution, and embedded in paraffin. Haematoxylin and eosin staining and immunohistochemistry analysis were performed by pathologists. All pathological examinations were performed by a team of pathologists who were blinded to the CT findings.

Image acquisition

All CT examinations were performed using a 16-section spiral CT system (GE Medical Systems, Milwaukee, WI, USA) or the newest dual-source detector CT (Siemens

Medical Systems, Erlangen, Germany). The imaging parameters were 120 kV, 250–300 mA. After administering 100ml iodinated contrast agent (300 mg iodine/ml) at a flow rate of 3 ml/s using a power injector, CT dynamic enhancement acquisition was performed at fixed time points. The protocol during the time period acquired was at 30 seconds for the arterial phase, 70 seconds for the portal venous phase, and 180 seconds for the equilibrium phase. Raw data were acquired and 5-mm axial images in the arterial phase were selected for texture analysis mainly for the clear delineation of lesions. Imaging data were retrieved from the Picture Archiving and Communication System (Centricity PACS Radiology RA1000 Workstation, General Electric, Milwaukee, WI, USA).

CT texture analysis

The arterial phase DICOM images of the largest cross-sectional area were exported to Omni-Kinetic software (GE Healthcare, Beijing, China) for texture analysis. The images were selected by a consensus reading of two radiologists with 10 years (GW) and 11 years (YXG) experience in abdominal imaging. ROIs were drawn as a polygon around the margins between the tumour and surrounding normal liver parenchyma by the same two radiologists. The ROI was positioned manually on the CT image for each patient (Fig 1). The texture parameters were automatically obtained by the software. Texture features derived from each lesion were as follows: first order, histogram, morphology metrics, grey-level co-occurrence matrix (GLCM), Haralick matrix, and run length matrix (RLM). Texture features represented the appearance of the medical images and the distribution of its pixel intensity. Various texture analysis approaches tend to represent the examined textures from different perspectives.[18] First order and histogram parameters were concerned with properties of individual pixels. They described the distribution of voxel intensities within the CT image through commonly used and basic metrics. Morphology included descriptors of the three-dimensional size and shape of the tumour region. The GLCM $\mathbf{P}(\mathbf{i}, |\theta, \mathbf{d})$ represented the joint probability of certain sets of pixels having certain grey-level values. It calculated how many times a pixel with grey-level i occurs jointly with another pixel having a grey value j, by varying the displacement vector d between each pair of pixels. Haralick measured the degree of similarity of the grey level of the image in the row or column direction. It represented the local grey level correlation, the greater its value, the greater the correlation. The grey-level RLM ($\mathbf{i}, \mathbf{j}|$) was defined as the numbers of runs with pixels of grey-level i and run length j for a given direction θ.

Statistical analysis

Statistical analysis was performed using the Statistical Package for Social Science version 20.0 (SPSS, Chicago, IL, USA). Independent Student's *t*-tests were used to compare continuous variables (patient age and maximum diameter of the lesions) between the different groups. Fisher's exact tests were used to compare categorical variables (sex of the patients). Kruskal–Wallis and Mann–Whitney tests were used to analyse the texture features of different groups. A *p*-value of <0.05 was considered to indicate statistically significant differences. According to the different lesions classification group, Fisher's discriminant analysis (FDA) was used to estimate the total discriminant accuracy. The basic principle for determining the parameter of the discriminant function in FDA was the maximum covariance in one class, along with the minimum covariance between different classes.[19,20] To remove the redundancy between the texture features, Spearman's rank correlation was performed prior to FDA. When correlation between the different parameters was >90%, one of the parameters would be removed. After Spearman's rank correlation screening, all features were included in FDA and cross-validation was performed using the leave-one-out method. Binary logistic regression and receiver operating characteristic (ROC) curve analysis were used to assess the diagnostic performance of texture analysis of benign and malignant tumours.

Results

Ultimately, a total of 84 patients (40 women, 44 men; mean age: 48.1±14.4 years, range: 6–73 years) with 88 lesions were enrolled in the present study. Two patients had three lesions, FNH in one patient, and HA in another. The accessed lesions included 20 HCCs, 18 FNHs, 10 HAs, 20 haemangiomas, and 20 hepatic metastases. The demographic information of the patients is shown in Table 1. Because of the prevalence of malignant tumours in elderly individuals, the mean age of patients was statistically significantly different ($p<0.01$) between patients with benign and those with malignant tumours. No significant difference was observed in terms of patients' sex and the maximum diameter of the lesions. Of all metastatic lesions, eight originated from colorectal cancer, three from pancreas cancer, three from lung cancer, two from breast cancer, two from biliary system cancer, one from gastric cancer, and one from vaginal cancer. Histopathological results included 16 adenocarcinoma, two small cell carcinoma, one squamous cell carcinoma, and one neuroendocrine carcinoma.

In the present study, 76 texture parameters were obtained from each patient, involving first order ($n=14$), histogram ($n=15$), morphology metrics ($n=9$), GLCM ($n=13$), Haralick matrix ($n=9$), and RLM ($n=16$). Spearman's correlation coefficients were used to evaluate the correlations between each pair of texture parameters. Twenty-four parameters were selected as the most powerful predictive features for further statistical analysis, as shown in Table 2.

Fifteen texture features were significant differences between the five different histopathological types of all lesions, as follows: min intensity, max intensity, median intensity, volume count, range, skewness, kurtosis, uniformity, quantile 95, GLCM energy, inertia, correlation, min size, high grey level run emphasis, Haralick correlation. Results of all five different histopathological types of

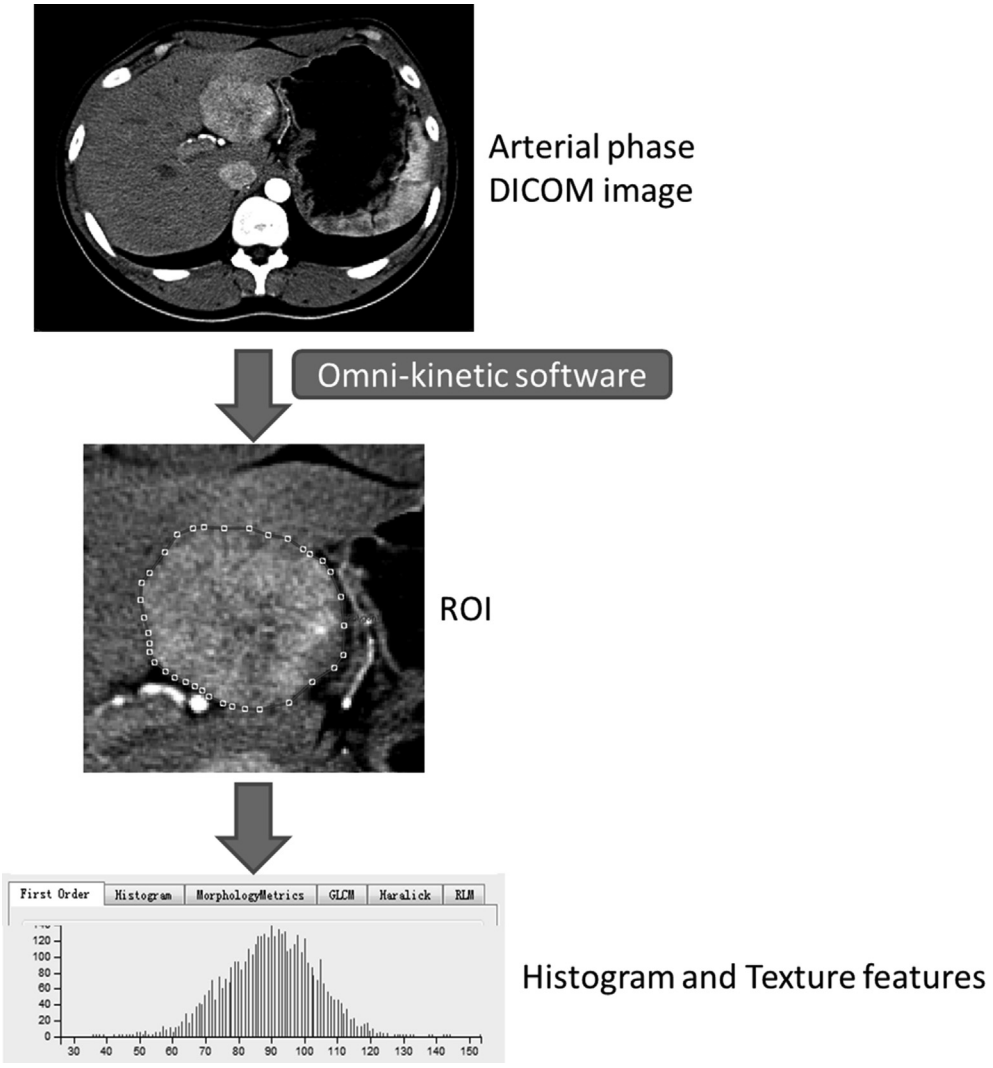

Figure 1 The steps of CT texture analysis. The arterial phase DICOM images of the largest cross-sectional area were exported to Omni-Kinetic software. The ROI was manually positioned on the CT image for each patient. The texture parameters were automatically obtained by the software.

Table 1
The demographic information of the patients.

	Total	Benign tumour[a]	Malignant tumour[b]	*p*-Value
Number	88	48 (10, 18, 20)	40 (20, 20)	
Sex (M/F)	49/40	20/28 (4/6, 7/11, 9/11)	29/11 (14/6, 15/5)	>0.05
Mean age (average±SD, years)	48.1±14.4	39.7±13.3 (36.1±13 31.7±10.3, 48.65±10.4)	57.2±8.3 (57.5±6.6, 47.6±14.3)	<0.001
Maximum diameter (average±SD, mm)	60.2±35.5	63.9±35.9 (52.9±29 41.9±20.9, 89.2±34.7)	55.9±34.8 (54.4±34.9, 60.2±35.5)	>0.05

[a] Focal nodular hyperplasia, hepatic adenoma and haemangioma.
[b] Hepatocellular carcinoma and metastases.

Table 2
Twenty-four parameters were selected by Spearman's correlation coefficients.

Calculation methods	Texture features
First order	Min intensity, max intensity, median intensity, volume count, range
Histogram	Skewness, kurtosis, uniformity, entropy, quantile 95
Morphology metrics	Sphericity
GLCM	GLCM energy, GLCM entropy, inertia, correlation, cluster prominence
RLM	Min size, max size, high grey-level run emphasis
Haralick	Haralick correlation, inverse difference moment, angular second moment, sum variance, difference entropy

GLCM, grey-level co-occurrence matrix; RLM, run length matrix.

tumour texture features are shown in Table 3. The total discriminant accuracy in the sample was 69.3%, with 55.7% cross-validation accuracy. A scatter plot of all five different types is shown in Fig 2.

All lesions were divided into two groups: benign tumours and malignant tumours. The benign tumours included FNH, HA, and haemangioma, while the malignant tumours included HCC and hepatic metastasis. Seven texture features showed significant differences between the two groups, including max intensity, range, kurtosis, quantile 95, min size, sum variance, and inverse difference moment. The FDA results of the two groups of tumour texture features are shown in Table 4. The total discriminant accuracy in the sample was 83%, with 77.3% cross-validation accuracy. To discriminate between the benign and malignant tumour groups, the area under the ROC curve (AUROC) of united texture features was 0.927 (95% confidence interval [CI]=0.875–0.979; Fig 3).

Discussion

The classification ability of texture analysis at the arterial phase of dynamic contrast-enhanced CT was investigated in hypervascular hepatic focal lesions, such as HCC, metastasis, haemangioma, HA, and FNH, and differentiating benign tumours from malignant tumours. There was a moderate discriminant accuracy (69.3% with 55.7% cross-validation accuracy) in the total samples, while a significant difference was seen between benign and malignant tumours with 83% discriminant accuracy and 77.3% cross-validation accuracy (AUROC 0.927).

Table 3
Total discriminant accuracy of five histopathological types tumour texture features.

Group	HAs *n* (%)	FNHs *n* (%)	Haemangiomas *n* (%)	HCCs *n* (%)	Metastases *n* (%)	Total
HAs	8 (80%)	0	0	1 (10%)	1	10
Cross-validation	5 (50%)	1 (10%)	0	3 (30%)	1 (10%)	
FNHs	3 (16.7%)	14 (77.8%)	0	1 (5.6%)	0	18
Cross-validation	4 (22.2%)	12 (66.7%)	0	2 (11.1%)	0	
Haemangiomas	0	1 (5%)	16 (80%)	1 (5%)	2 (10%)	20
Cross-validation	0	1 (5%)	14 (70%)	1 (5%)	4 (20%)	
HCCs	3 (15%)	1 (5%)	0	11 (55%)	5 (25%)	20
Cross-validation	4 (20%)	2 (10%)	2 (10%)	8 (40%)	4 (20%)	
Metastases	5 (25%)	0	0	3 (15%)	12 (60%)	20
Cross-validation	5 (25%)	0	1 (5%)	4 (20%)	10 (50%)	

The total discriminant accuracy in the sample was 69.3%, with 55.7% cross-validation accuracy.
FNH, focal nodular hyperplasia; HA, hepatic adenoma; HCC, hepatocellular carcinoma.

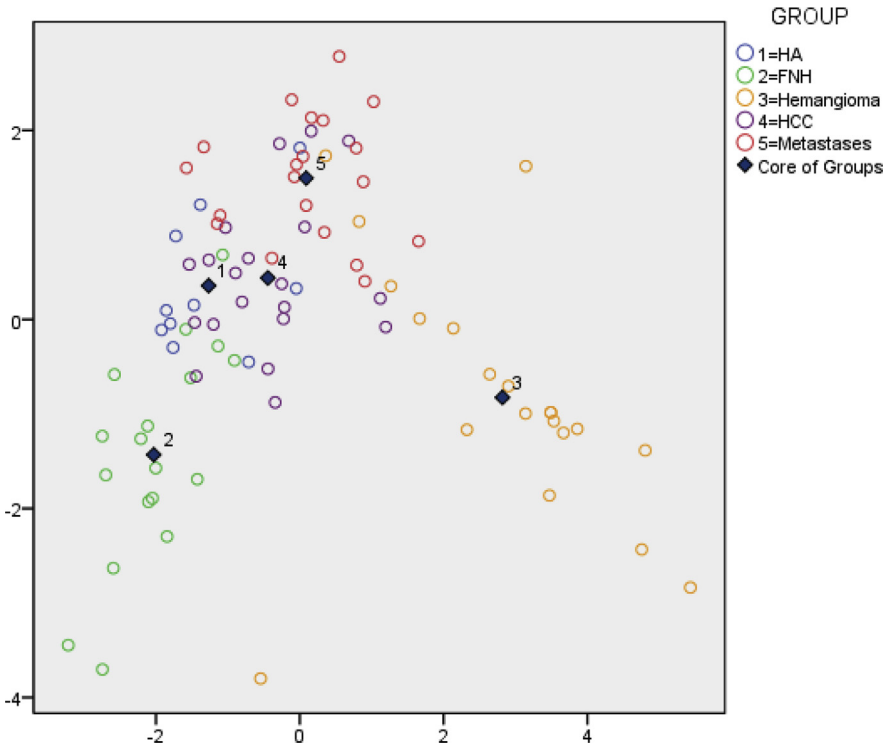

Figure 2 Scatter plot of texture features of the five types of tumor.

Table 4
Total discriminant accuracy of benign and malignant tumour texture features.

Group	Benign tumour *n* (%)	Malignant tumour *n* (%)	Total
Benign tumour	38 (79.2%)	10 (20.8%)	48
Cross-validation	35 (72.9%)	13 (27.1%)	
Malignant tumour	5 (12.5%)	35 (87.5%)	40
Cross-validation	7 (17.5%)	33 (82.5%)	

The total discriminant accuracy in the sample was 83%, with 77.3% cross-validation accuracy.
FNH: focal nodular hyperplasia; HA: hepatic adenoma; HCC: hepatocellular carcinoma.

Multi-spiral dynamic contrast-enhanced CT is currently the main method used for examination of tumour diagnosis. It is widely used in the differential diagnosis of focal hepatic lesions, and can provide information about the blood supply of the lesions. HCC, metastasis, haemangioma, HA, and FNH are hypervascular hepatic focal lesions, which manifest similar obvious enhancement at arterial phase in dynamic contrast-enhanced CT.[16] Some cases may not be distinguished correctly by radiologists because of the atypical manifestations of these hepatic tumours; however, analysis of the texture features could provide primary or additional information, which is related to the biological nature of the lesions and beyond visual inspection.[17,21] In addition to practical considerations, the margins of hypervascular hepatic lesions at the arterial phase are distinct, so it will be more precise to draw the ROI by hand than on portal venous or equilibrium phase scans.[22] Therefore, the arterial phase was chosen for the texture-based differential diagnosis of focal hepatic lesions.

Tumours are heterogeneous at the histopathological level, which lead to disorganised growth patterns and a heterogeneous appearance in imaging examinations. For this reason, some previous studies used texture analysis for diagnosis and examination of different hepatic lesion types. For example, Huang *et al.*[21] examined 164 liver lesions on unenhanced CT, using a form of texture analysis for distinguishing between benign haemangiomas and malignant hepatic tumours, and found that it had an accuracy of 81.7% in identifying malignancies. Further exploration of the utility of texture analysis in the realm of diagnostic assistance and tissue characterisation could theoretically be used by radiologists at the workstation in future. In the present study, while the differentiation of traditional hypervascular lesions (i.e., HCC, HA, FNH) can usually be performed by taking into account their characteristic multiphase CT appearances, employing CT texture analysis as an auxiliary diagnostic tool in cases with hypervascular hepatic lesions could be of great value, if rigorously studied and judiciously applied.

Distinguishing between benign and malignant solid lesions of the liver by means of texture analysis can avoid unnecessary invasive treatment.[23] Gletsos *et al.*[24] evaluated the use of a computer-aided diagnostic system for the classification of hepatic lesions from non-enhanced CT images of normal liver, hepatic cysts, haemangiomas, and HCCs, resulting in a minimum error rate of 15.79%. They used three sequentially placed feed-forward neural networks (NNs) for classifying liver disease, the third NN distinguished haemangioma and HCC. The best classification rate was 91%, obtained for the validation set by using four features selected using a genetic algorithm-based search. Raman *et al.*[22] used CT texture analysis software

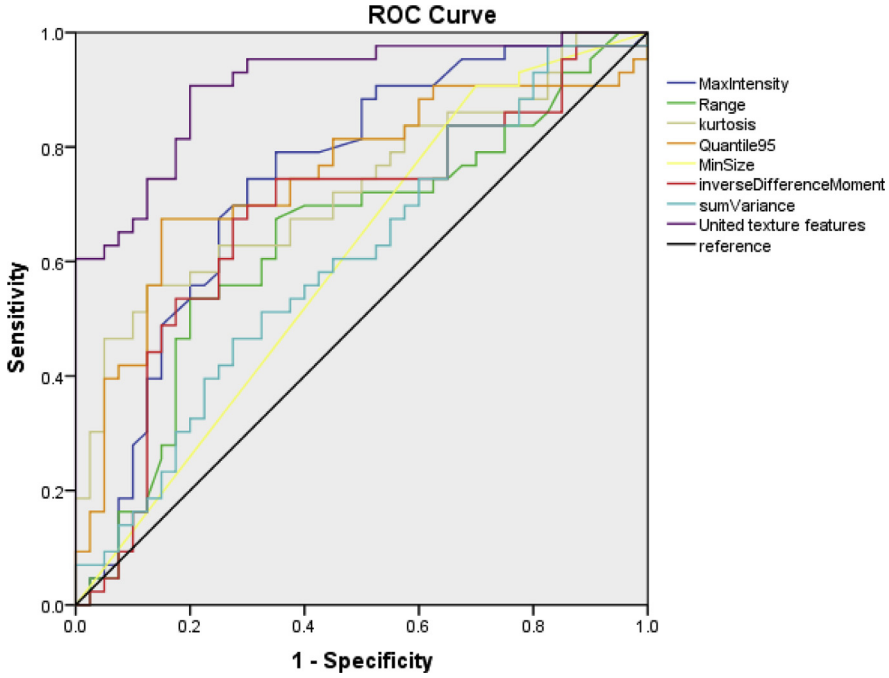

Figure 3 ROC analysis of texture features in the differential diagnosis of benign and malignant tumors.

with random-forest statistical modelling to analyse FNH, HA, HCCs, and normal liver parenchyma using arterial phase scans. The model's error rates were only 11.2%, 20.9%, 7.2%, and 2.1%, respectively. They found the error rate of either being "benign" (i.e., normal liver, FNH, HA) or "malignant" (i.e., HCC) was 21.8%. In their study, the differentiation and classification of a small subset of hypervascular hepatic lesions was lower; however, the validation of their technique was insufficient. In the present study, five types of hypervascular hepatic lesions, which confirmed at histopathology, were assessed. The total discriminant accuracy in the sample was 69.3%, with 55.7% cross-validation accuracy between the five different histopathological types of all lesions. Then when all lesions were separated into benign and malignant tumours, the total discriminant accuracy for benign and malignant tumour samples was 83%, with 77.3% cross-validation accuracy. The AUROC of united texture features was 0.927 (95% confidence interval [CI]= 0.875–0.979). This indicated that the CT texture analysis was highly accurate for identification of benign and malignant tumours among solid liver lesions. Kamel *et al.*[25] assessed the diagnostic accuracy of focal hepatic lesions on dual-phase helical CT by three experienced radiologists. The AUROC was 0.84, 0.83, and 0.85, respectively, which were lower than that of the present study (0.927). It showed that texture analysis could improve the diagnostic accuracy to a certain extent. The present study of CT texture analysis was undertaken to aid diagnosis by radiologists. Although this was only a pilot study, examining a small number of different lesion types with relatively small sample sizes, the results of the FDA and AUROC suggested the potential of CT texture analysis for lesion characterisation when combined with appropriate statistical modelling. In particular, unlike previous studies of CT texture analysis in lesion characterisation, the results of this study demonstrated the superiority of models utilising a combination of most powerful different texture features, rather than simply concentrating on pairwise comparisons of individual parameters.

There are several limitations of the present study that should be acknowledged. First, it was retrospective in nature and contained some selection bias because all the patients investigated were candidates for surgery or liver percutaneous needle biopsy. For example, most of the haemangiomas targeted for surgery in the present cohort were larger, and presented as globular or nodular peripheral enhancements, similar to attenuation of blood vessels in the arterial phase; however, smaller haemangiomas showing homogeneous enhancement in the arterial phase, which were diagnosed easily using dynamic CT, did not require surgical intervention, and were excluded from the present study. Second, the present study was a pilot study examining the classification of five categories of hypervascular hepatic lesions. All lesions were histopathologically demonstrated, but the number of FNH and HA were insufficient and the total sample size of patients in the study was inadequate. More patients should be recruited for CT texture analysis in future. Third, in the present study, several types of CT machines from different suppliers were used. To standardise the protocols for obtaining images, imaging parameters and CT dynamic enhancement acquisition time were the same, and 5-mm axial images were selected for texture analysis. Nonetheless, variations in acquisition and image reconstruction parameters for CT texture analysis could introduce differences that were not due to biological effects.[26] Fourth, segmentation of the tumours was challenging, some tumours were vague, and it was not easy to distinguish the borders between the tumour and the normal liver parenchyma. To address this, ROIs were drawn by two experienced radiologists. Some patients were excluded because the ROI diameter was $<$10 mm and the margin of the lesion was indistinct, making it unsuitable for drawing an ROI.

In conclusion, tumours that manifest similar imaging features may have different histopathologic diagnosis. Texture analysis provides quantitative measures for tumour lesion discrimination and characterisation based on the distribution of pixel intensities at different spatial frequencies. Texture analysis based on CT images can be used as an aid in the differential diagnosis of hypervascular solid focal hepatic lesions, especially the differential diagnosis between benign and malignant lesions. To assist with diagnostic classification, this strategy for quantitative analysis of texture features merits further exploration.

Conflict of interest

The authors declare no conflict of interest.

Acknowledgements

This study was funded by Current Funding Sources: Natural Science Foundation of Shandong Province (ZR2017BH044).

References

1. Lambin P, Rios-Velazquez E, Leijenaar R, *et al*. Radiomics: extracting more information from medical images using advanced feature analysis. *Eur J Cancer (Oxford, England: 1990)* 2012;**48**(4):441–6. https://doi.org/10.1016/j.ejca.2011.11.036.
2. Kumar V, Gu Y, Basu S, *et al*. Radiomics: the process and the challenges. *Magn Reson Imaging* 2012;**30**:1234–48. https://doi.org/10.1016/j.mri.2012.06.010.
3. Parekh V. Radiomics: a new application from established techniques. *Expert Rev Precis Med Drug Dev* 2016;**1**:207–26. https://doi.org/10.1080/23808993.2016.1164013.
4. Gillies RJ, Kinahan PE, Hricak H. Radiomics: images are more than pictures, they are data. *Radiology* 2015;**278**(2):151169. https://doi.org/10.1148/radiol.2015151169.
5. Castellano G, Bonilha L, Li LM. Texture analysis of medical images. *Clin Radiol* 2004;**59**(12):1061–9. https://doi.org/10.1016/j.crad.2004.07.008.
6. Hahn S, Heusner T, Zhou X, *et al*. Computer-aided detection (CAD) and assessment of malignant lesions in the liver and lung using a novel PET/CT software tool: initial results. *RöFo* 2010;**182**(03):243–7. https://doi.org/10.1055/s-0028-1109833.
7. House MJ, Bangma SJ, Thomas M, *et al*. Texture-based classification of liver fibrosis using MRI. *J Magn Reson Imaging* 2015;**41**(2):322–8. https://doi.org/10.1002/jmri.24536.
8. Ba-Ssalamah A, Muin D, Schernthaner R, *et al*. Texture-based classification of different gastric tumours at contrast-enhanced CT. *Eur J Radiol* 2013;**82**(10):e537–43. https://doi.org/10.1016/j.ejrad.2013.06.024.

9. Van Ginneken B, Romeny BMTH, Viergever MA. Computer-aided diagnosis in chest radiography: a survey. *IEEE Trans Med Imaging* 2001;**20**(12):1228–41. https://doi.org/10.1109/42.974918.
10. Alobaidli S, McQuaid S, South C, *et al*. The role of texture analysis in imaging as an outcome predictor and potential tool in radiotherapy treatment planning. *Br J Radiol* 2014;**87**(1042):20140369. https://doi.org/10.1259/bjr.20140369.
11. Gourtsoyianni S, Papanikolaou N, Yarmenitis S, *et al*. Respiratory gated diffusion-weighted imaging of the liver: value of apparent diffusion coefficient measurements in the differentiation between most commonly encountered benign and malignant focal liver lesions. *Eur Radiol* 2008;**18**(3):486–92. https://doi.org/10.1007/s00330-007-0798-4.
12. Nicolau C, Vilana R, Catalá V, *et al*. Importance of evaluating all vascular phases on contrast-enhanced sonography in the differentiation of benign from malignant focal liver lesions. *AJR Am J Roentgenol* 2006;**186**(1):158–67. https://doi.org/10.2214/AJR.04.1009.
13. Boas FE, Kamaya A, Do B, *et al*. Classification of hypervascular liver lesions based on hepatic artery and portal vein blood supply coefficients calculated from triphasic CT scans. *J Digit Imaging* 2015;**28**(2):213–23. https://doi.org/10.1007/s10278-014-9725-9.
14. Ichikawa, Federle MP, Grazioli L, *et al*. Hepatocellular adenoma: multiphasic CT and histopathologic findings in 25 Patients. *Radiology* 2000;**214**(3):861–8. https://doi.org/10.1148/radiology.214.3.r00mr28861.
15. Carlson SK, Johnson CD, Bender CE, *et al*. CT of focal nodular hyperplasia of the liver. *AJR Am J Roentgenol* 2000;**174**(3):705–12. https://doi.org/10.2214/ajr.174.3.1740705.
16. Ganeshan B, Panayiotou E, Burnand K, *et al*. Tumour heterogeneity in non-small cell lung carcinoma assessed by CT texture analysis: a potential marker of survival. *Eur Radiol* 2012;**22**(4):796–802. https://doi.org/10.1007/s00330-011-2319-8.
17. Nakashima Y, Nakashima O, Hsia CC, *et al*. Vascularization of small hepatocellular carcinomas: correlation with differentiation. *Liver Int* 1999;**19**(1):12–8. https://doi.org/10.1111/j.1478-3231.1999.tb00003.x.
18. Chiang LH, Russell EL, Braatz RD. Fault diagnosis in chemical processes using Fisher discriminant analysis, discriminant partial least squares, and principal component analysis. *Chemometr Intell Lab* 2000;**50**(2):243–52. https://doi.org/10.1016/S0169-7439 (99)00061-1.
19. Ostrovsky E, Zelig U, Gusakova I, *et al*. Detection of cancer using advanced computerized analysis of infrared spectra of peripheral blood. *IEEE Trans Bio-Med Eng* 2013;**60**:343–53. https://doi.org/10.1109/TBME.2012.2226882.
20. Dong L, Sun X, Chao Z, *et al*. Evaluation of FTIR spectroscopy as diagnostic tool for colorectal cancer using spectral analysis. *Spectrochim Acta A* 2014;**122**:288–94. https://doi.org/10.1016/j.saa.2013.11.031.
21. Huang YL, Chen JH. Diagnosis of hepatic tumours with texture analysis in nonenhanced computed tomography images. *Acad Radiol* 2006;**13**(6):713–20. https://doi.org/10.1016/j.acra.20.
22. Raman SP, Schroeder JL, Huang P, *et al*. Preliminary data using computed tomography texture analysis for the classification of hypervascular liver lesions: generation of a predictive model on the basis of quantitative spatial frequency measurements—a work in progress. *J Comput Assist Tomogra* 2015;**39**(3):383–95. https://doi.org/10.1097/RCT.0000000000000217.
23. Taylor HM. Hepatic imaging: an overview. *Radiol Clin N Am* 1998;**36**(2):237–45. https://doi.org/10.1016/S1089-3261 (03)00063-1.
24. Gletsos M, Mougiakakou SG, Matsopoulos GK, *et al*. A computer-aided diagnostic system to characterize CT focal liver lesions: design and optimization of a neural network classifier. *IEEE Trans Inf Technol B* 2003;**7**(3):153–62. https://doi.org/10.1109/TITB.2003.813793.
25. Mackin D, Fave X, Zhang L, *et al*. Measuring computed tomography scanner variability of radiomics features. *Invest Radiol* 2015;**50**(11):757–65. https://doi.org/10.1097/RLI.0000000000000180.
26. Kamel IR, Choti MA, Horton KM, *et al*. Surgically staged focal liver lesions: accuracy and reproducibility of dual-phase helical CT for detection and characterization. *Radiology* 2003;**227**(3):752–7. https://doi.org/10.1148/radiol.2273011768.